Available online at www.sciencedirect.com

ScienceDirect

Physics Procedia 89 (2017) 11 – 22

Physics Procedia

Nordic Laser Materials Processing Conference, NOLAMP_16, 22-24 August 2017, Aalborg University, Denmark

Hybrid welding of 45 mm high strength steel sections

Ivan Bunaziv[a]*, Jan Frostevarg[b], Odd M. Akselsen[a,c], Alexander F. Kaplan[b]

[a] *Norwegian University of Science and Technology, Department of Engineering Design and Materials, Richard Birkelands vei 2B, NO-7043 Trondheim, Norway*

[b] *Luleå University of Technology, Department of Engineering Sciences and Mathematics, SE-97187 Luleå, Sweden*

[c] *SINTEF Materials and Chemistry, P.O. Box 4760 Sluppen, NO-7465 Trondheim, Norway*

Abstract

Thick section welding has significant importance for oil and gas industry in low temperature regions. Arc welding is usually employed providing suitable quality joints with acceptable toughness at low temperatures with very limited productivity compared to modern high power laser systems. Laser-arc hybrid welding (LAHW) can enhance the productivity by several times due to higher penetration depth from laser beam and combined advantages of both heat sources. LAHW was applied to join 45 mm high strength steel with double-sided technique and application of metal cored wire. The process was captured by high speed camera, allowing process observation in order to identify the relation of the process stability on weld imperfections and efficiency. Among the results, it was found that both arc power and presence of a gap increased penetration depth, and that higher welding speeds cause unstable processing and limits penetration depth. Over a wide range of heat inputs, the welds where found to consist of large amounts of fine-grained acicular ferrite in the upper 60-75% part of welds. At the root filler wire mixing was less and cooling faster, and thus found to have bainitic transformation. Toughness of deposited welds provided acceptable toughness at -50 °C with some scattering.

Peer-review under responsibility of the scientific committee of the Nordic Laser Materials Processing Conference 2017

Keywords: hybrid welding; high strength low alloy steel; thick section; acicular ferrite; toughness

* Corresponding author. Tel.: +47-45795269.
E-mail address: ivan.bunaziv@ntnu.no

Peer-review under responsibility of the scientific committee of the Nordic Laser Materials Processing Conference 2017
doi:10.1016/j.phpro.2017.08.006

1. Introduction

Fusion welding is an essential manufacturing process used in heavy industry where 10-60 mm thick plates are frequently used. Thick section welding is of great interest, in recent years, for low temperature applications. A well-established arc technique, such as metal active gas (MAG) welding is commonly used for this task. However the process has limited welding speeds and overall productivity compared to the laser beam welding (LBW) technology. Modern fiber laser beam technology with high powers offers much higher production rates due to higher penetration depth (Ono et al., 2002). By adding MAG process to LBW, making so-called laser-arc hybrid welding (LAHW), the productivity can be increased even further with ability to manipulate microstructure though added filler wire (Moore et al., 2004) and moderate cooling rates which are extremely important for achieving acceptable toughness at low temperatures by facilitating high amount of acicular ferrite (Svensson and Gretoft, 1990). LAHW using a fiber laser is reported by a few research groups in providing good results in achieving toughness. Grünenwald et al. (2010) applied LAHW on 9.5 mm high strength steel (HSS) with high welding speeds, at 2 m/min, high impact toughness (more than 100 J) at -20 °C was achieved. Joining 8-12 mm root in 20-23.4 mm X80 and X120 high strength steel by LAHW with modified spray arc process, by using both solid and metal cored electrode, provided excellent impact toughness even at -60 °C giving 190 J on average (Gook et al., 2014). First attempts by Akselsen et al. (2014) to weld 20 mm structural HSS by using keyhole LAHW provided reasonable impact toughness only at -30 °C due to high cooling cycles in the middle of the plate consisting of bainitic-martensitic microstructural development. Pan et al. (2015) performed one-pass welding of 11 mm HSS, where joints had minimum of 150 J impact toughness at -40 °C.

A relatively new cold metal transfer plus pulsed (CMT+P) arc mode, characterized as short-circuiting phase combination with pulsing, providing significantly lower the heat input (Pang et al., 2016) than standard Pulsed arc mode. The usage of CMT+P in combination with metal cored wire can be a perspective arc mode and overall improvement used for joining thick high strength low alloy steel sections by combining it with fiber laser to form hybrid welding process. Such combination applied for thick steel section welding was not reported.

In this paper, 45 mm HSS was joined by deep penetration LAHW, in double-sided technique, with acceptable weld quality and toughness at -50 °C as a partial penetration joints due to lack of fusion in most of welds. The stability of the process was observed by high speed camera in order to understand the effect of various welding parameters and generated imperfections. Testing a wide range of parameters including different arc modes (CMT+P/Pulsed), air gaps, travel speeds, filler wire feed rates (arc power) and torch arrangement revealed that upper part of welds had favorable microstructural development whereas at the root bainite was commonly observed related to difficulties of filler wire delivery and substantial increased cooling cycles.

2. Methodology

The LAHW setup is illustrated in Fig. 1a, where a 15 kW IPG Laser YLR-15000 ytterbium fiber laser (wavelength 1070 nm) was applied. The laser had a fiber core diameter of 400 μm, beam parameter product 10.3 mm·mrad, was operating in continuous wave mode and focused below the surface (-7 mm focal spot position) by 300 mm focal length optics to a spot size of 800 μm diameter with resulting Rayleigh length ±4 mm was applied. The laser was combined with MAG welding equipment TPS4000 VMT Remote from Fronius GmbH. The wire feeder is a combination of a continuous feeding unit VR7000 with a Robacta Drive unit that carries out the back and forth motion of the wire tip which enables the CMT process used in the experiments. To prevent high back reflections damaging the optical fiber, a slight tilting of 7° of the laser was applied. The MAG torch had the angle of 60±2° and 15±1 mm distance to the surface of specimen. Argon with 18% CO_2 shielding gas mixture was used with 25 L/min flow rate. The welds were carried out using an articulated robot from Motoman.

45 mm thick high strength steel plates (yield strength of 500 MPa) was used in the experiments and chemical composition is shown in Table 1. The plates were plasma cut by 500x125 mm and edges were milled for welding. The upper part near weld edge was sandblasted. The workpieces were fixed with heavy clamping system. Filler wire used was a metal cored wire Kobelco Trustarc MX-A55T of 1.2 mm in diameter with chemical composition presented in Table 1. High speed imaging (HSI) camera (Redlake) was used from the side, tilted by 55° from the horizontal (normal) surface. Region of interest had the resolution of 800x600 pixels with 10 bits pixel depth. Illumination pulsed

laser (Cavitar) with 500 watt peak power during 3 µm shutter exposure time was used in order to increase the quality of the captured images. A band pass filter was applied to suppress process light with matching the wavelength (808 nm) to an illumination diode laser. 3410 frames per second were captured for each experiment with approx. 1.2 s filming duration. A detailed arrangement of the equipment is shown in Fig. 1b.

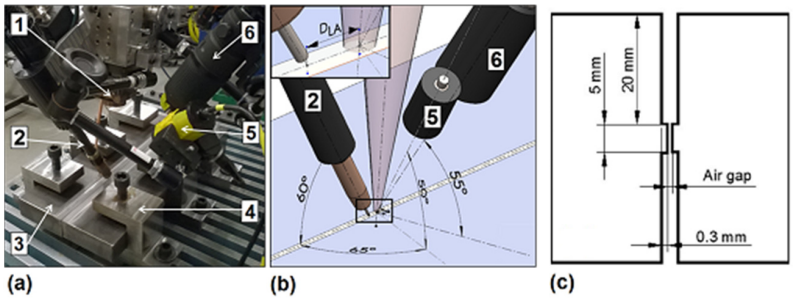

Fig. 1. (a) and (b) is experimental set-up: 1 – fiber laser equipment; 2 – MAG equipment; 3 – steel workpieces; 4 – heavy clamping system; 5 – illumination pulsed diode laser; 6 – high speed imaging camera; (c) gap preparation of plates.

Table 1. Chemical compositions (wt. %) of base material and filler wire. Iron (Fe) in balance.

Material	C	Si	Mn	P	S	Al	Nb	V	Ni	Ti	Cr	Cu	Mo
Base material	0.036	0.082	1.97	0.007	0.001	0.025	0.01	0.01	0.7	0.008	0.07	0.18	0.1
Trustarc MX-A55T	0.06	0.35	1.41	0.011	0.017	-	-	-	1.48	-	-	-	-

A constant 15 kW laser beam power was applied and using 4-5 mm laser-arc interdistance (D_{LA}) and schematically shown in Fig. 1b. The most rational double-sided welding technique was chosen for joining steel plates where for two runs, the first run is top weld seam and the second run is bottom weld seam, the same welding parameters were applicable. Variables significantly affecting the process stability and efficiency changed between experimental runs are presented in Table 2. Total line energy output for LAWH (Q_H, kJ/mm) is calculated as a sum of laser beam (Q_L, kJ/mm) and arc energy (Q_A, kJ/mm) outputs:

$$Q_H = Q_L + Q_A = \frac{60 \cdot P}{v_t} + \frac{60 \cdot I \cdot V}{1000 \cdot v_t} \quad (1)$$

where P – laser power (kW); I – current (A); V – voltage (V); and v_t – travel speed (mm/min).

The arc parameters such as current, voltage, and pulsing characteristics were set according to the Fronius GmbH synergetic lines for Pulsed and CMT+P modes and depends on filler wire feed rate (*WFR*).

Table 2. Variable welding parameters of the experimental runs.

Weld number	Air gap, mm	Travel speed, m/min	Filler wire feed rate, m/min (output power)	Arc mode	Torch arrangement	Total line energy output, kJ/mm
1	0.3	0.6	7.0 (2.8 kW)	CMT+P	Trailing	1.8
2	0.3	0.6	7.0 (5.3 kW)	Pulsed	Trailing	2.0
3	0.3	0.6	7.0 (2.7 kW)	CMT+P	Leading	1.8
4	0.3	0.6	7.0 (5.6 kW)	Pulsed	Leading	2.1
5	0.8	0.8	10.0 (5.1 kW)	CMT+P	Trailing	1.5
6	0.8	0.8	10.0 (7.2 kW)	Pulsed	Trailing	1.7
7*	0.4	0.8	9.0 (4.1 kW)	CMT+P	Trailing	1.4
8	0.4	0.8	9.0 (6.9 kW)	Pulsed	Leading	1.7

9	0.6	0.6	7.0 (2.6 kW)	CMT+P	Trailing	1.8
10	1.0	1.2	18.0 (12.9 kW)	Pulsed	Trailing	1.4
11**	0.4	0.8	9.0 (6.9 kW)	CMT+P	Leading	1.4

* 2.5-3 mm process distance due to technical issues was applied for 1st pass

** no impact toughness testing was performed for this welded specimen

The bevelling geometry in edge preparation plates is a square which is straight edge with a 5 mm nose presented in Fig. 1c. Droplet transfer stability, interaction between arc and laser beam, keyhole stability and melt flow analysed through HSI as shown from trailing arc in Fig. 2a and for leading arc arrangement Fig 2b.

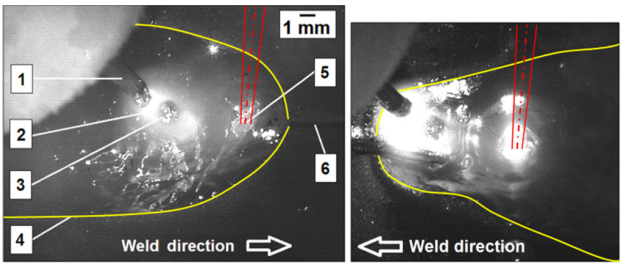

Fig. 2. HSI of laser-MAG hybrid welding for (a) trailing torch arrangement and (b) leading torch arrangement where: 1 – filler wire, 2 – arc plasma, 3 – molten droplet, 4 – liquid weld pool rim, 5 – laser keyhole, 6 – air gap between plates.

A series of destructive mechanical testing was performed to identify mechanical properties of welds including macrosections, hardness testing and Charpy V-notch toughness testing at -50 °C (3 specimens). The hardness of the welded joints, in accordance with ISO 9015-2 (HV 2 micro hardness), was measured across the weld beads in two lines. The first line was situated 3 mm below the upper surface and the second line 2 mm above the maximum penetration depth from the root. Charpy V-notch specimens with the standard specimen dimensions 10x10x55 mm were machined and intended notch was positioned on the fusions line (FL) and weld metal (WM) so that the crack propagates parallel to weld direction providing the lowest possible toughness values therefore increasing reliability of the design. The notch was located on one of the produced runs.

3. Results and discussion

3.1. Process stability and efficiency

Two HSI videos were available for the each welding run with equal set of parameters since two-side welding technique was used and in most of the cases both videos show identical process behaviour. As a result, the findings are more reliable due to some repeatability.

A combination of trailing CMT+P arc mode with high power 15 kW laser beam was stable at 0.6 m/min in selected range of welding parameters. For stability representation the streak image was implied as shown in Fig. 3a (weld No. 1) where the process is characterized by double pulsing with a subsequent CMT phase afterwards where a formed droplet deposited by short-circuiting method (physical direct electrode or filler wire contract with molten metal pool). A more detailed explanation about streak image technique is given by Frostevarg et al. (2014) applied for hybrid welding process where different arc modes are studied. The process was also facilitated by one-droplet-per-pulse (ODPP) with straight molten droplet flight path trajectory deposition. By increasing travel speed to 0.8 m/min, and slight increase of WFR of 2.0 m/min, sometimes a destabilization phenomenon called wire chopping occurred, which is characterized as a whole filler wire cut (see Fig. 3b, weld No. 7) that usually introduced severe spattering or even macro-porosity (see Fig. 4d). Wire chopping occurrence is rather seldom (about 4-5 times per 1.2 s of processing that lasts only about 15 ms) and generated due to extremely short arc in relation to wire susceptibility for arc to propagate inside the wire. This regularly occurred in the middle of pulsing (e.g. if six pulses present, after the 2nd or 3rd pulse

wire chopping occurs), but rarely in the beginning or on the last pulse before short-circuiting phase. This destabilization is more common for CMT+P arc mode, due to also improper retraction of wire after short-circuiting phase resulting in very short arc length (Fig. 3b$_{iii}$), and implies that in Pulsed arc mode it occurs more rarely due to absence of this phase. Longer arc length had better rooting effect (the arc ability and stability continuously melting base material) especially when stronger arc was applied (Sugino et al., 2005). Leading torch arrangement is more resistant to wire chopping (see Fig. 5d, weld No. 11) due to a deeper arc gouge which has lower molten metal level inside the gouge.

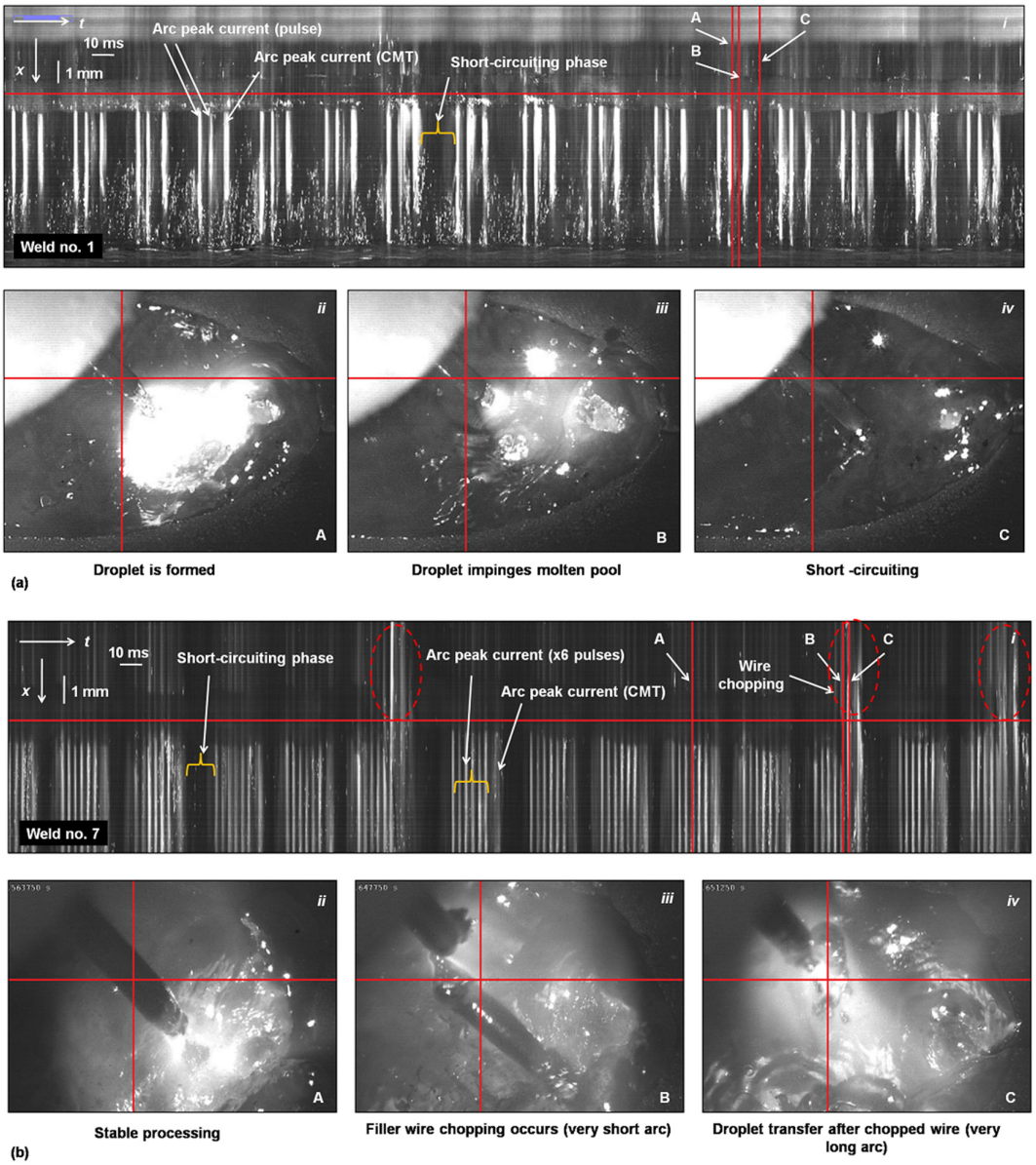

Fig. 3. HSI (55° inclination from the normal) analysis of LAHW with stable processing (a) and (b) unstable processing with wire chopping destabilization, where *i* is a streak image of each for a selected line and *ii*-*iv* are relevantly selected frames.

As a result, in order to avoid wire chopping and facilitate higher travel speeds, leading pulsed arc is recommended with higher filler wire feed rate since higher arc power provides better rooting effect. Moreover, leading torch arc is

more concentrated (voltage is decreased and current was increased by 5% according to the obtained data). An increase of arc power, filler wire feed rate, mitigates wire chopping and enables welding with higher travel speeds (up to 1.2 m/min in present studies). However, a such high travel speeds even with a sufficient filler wire feed rate (18 m/min for weld No. 10 used) significant underfill is produced (Fig. 4j) as well other experiments with increased of air gap to 0.8 mm produces undercuts (Fig. 4c, h) and filler wire feed rate should be increased as well.

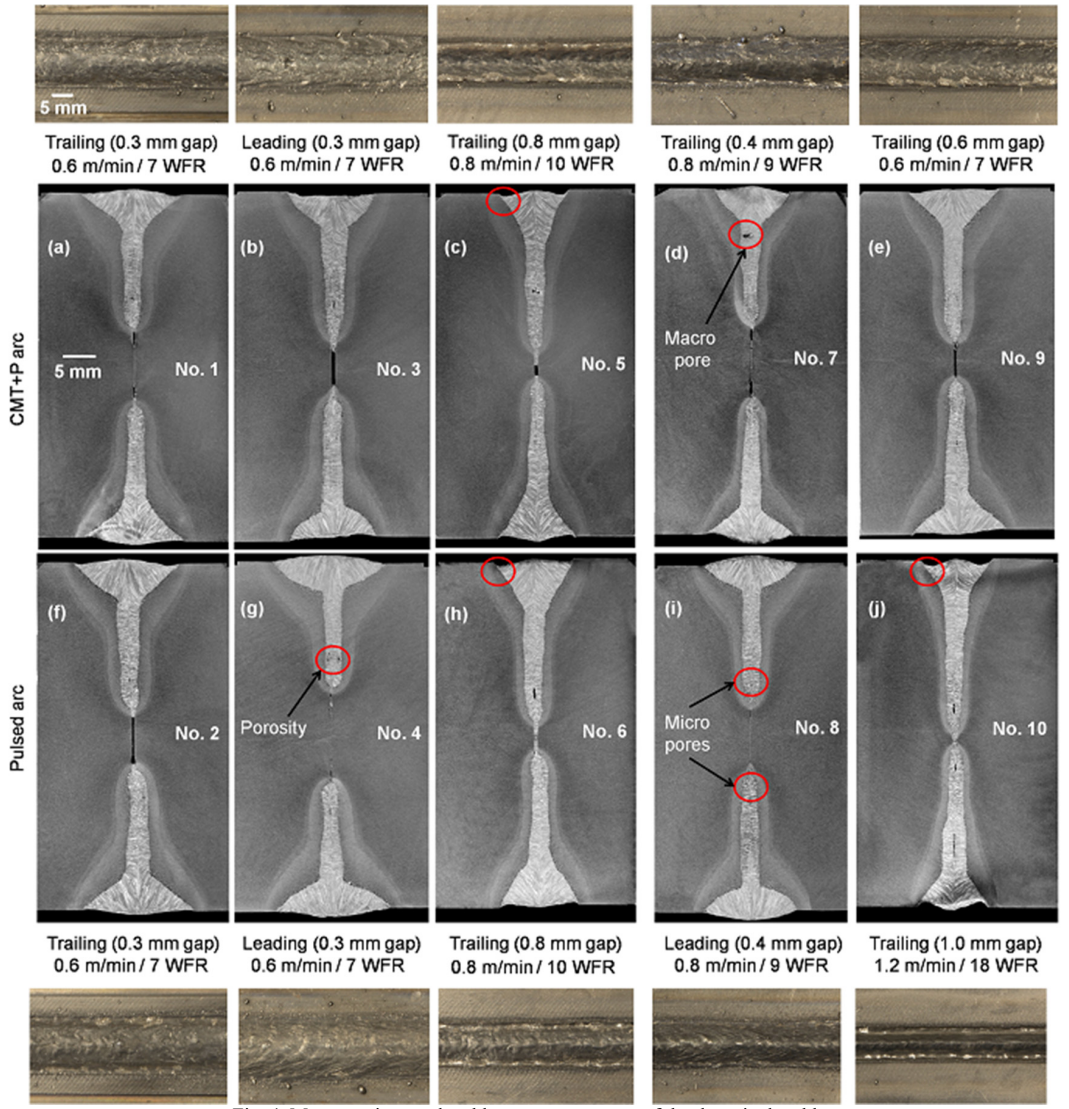

Fig. 4. Macrosections and weld seam appearances of the deposited welds.

Leading pulsed torch arrangement tends to produce porosity (Fig. 4g) due to unfavorable droplet trajectory which is changed towards the keyhole (Fig. 5b**,** weld No. 4) with 7 m/min feed rate having multiple-droplet-per-pulse (MDPP) transfer and therefore resulting in poorer surface quality (see Fig. 4b, g) compared to trailing torch arrangement which had droplet path trajectory changed from the keyhole (Fig. 5a, weld No. 2). The trajectory became more changed with increasing arc power that possess spray metal transfer with significantly smaller droplets than wire diameter (Fig. 5c, weld No. 8) and resulted in micro-porosity (Fig. 4i) since they hit the keyhole more frequently.

CMT+P provided lower droplet trajectory flight path change magnitude and therefore porosity was reduced (Fig. 5b) due to better control over pinch-effect (ODPP) for both torch arrangements.

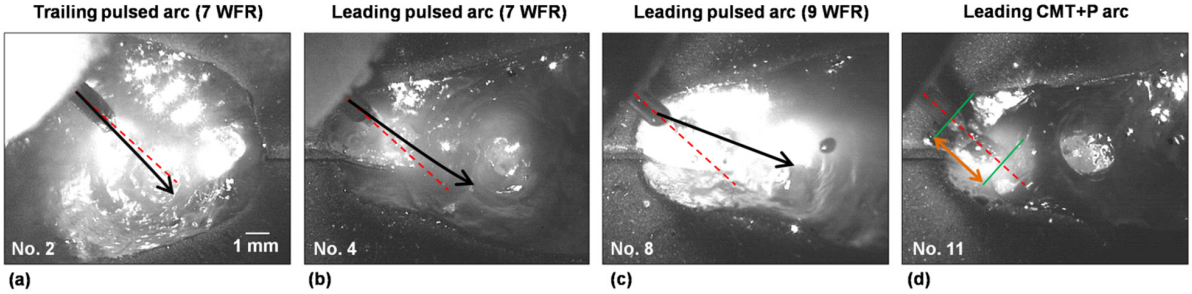

Fig. 5. HSI frames (55° inclination from the normal) of trajectory path change of the deposited droplet (a, b, c) and increased arc length for leading CMT+P arc (d).

Most experimental runs achieved a penetration depth in the range of 16-21 mm from each side (32-42 mm corresponding thickness for double-sided technique). Fig. 6 shows the measured penetration depths for the different welds. The air gap and arc power (for corresponding *WFR*) were very effective to improve penetration depth, or process efficiency, significantly even though travel speed was increased. However, with increase of travel speed the air gap and arc power correspondingly. Air gap provides a possibility to increase penetration depth and therefore travel speed can be increased to increase overall productivity. By using CMT+P arc mode the penetration depth is decreasing with increase of travel speed and that could be related to the stability of the process due to wire chopping phenomena. CMT+P arc mode in the range at travel speed 0.6 m/min (with stable processing) provided similar penetration depth but had lower heat input (see Table 2) that offers economic advantage and possibly less distortions.

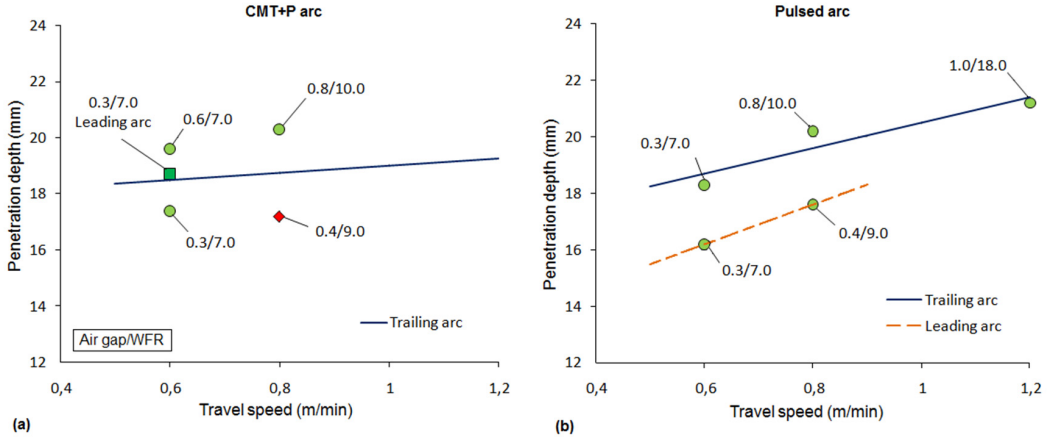

Fig. 6. Penetration depth depending on arc mode, travel speed, air gap, torch arrangement, and filler wire feed rate (WFR) where the data point shape represent the stability: rhomb (♦) – unstable process with wire chopping and explosive metal transfer; circle (●) – relatively stable process; and square (■) – stable process.

3.2. Microstructural development and mechanical properties of the deposited welds

Base material of low carbon steel was consisting of ferrite matrix with very small bainitic islands, precipitates within the ferrite matrix grains and some grain boundary carbides between ferrite grains (Fig. 8a). Deposited welds consisted of large amount of fine-grained acicular ferrite (AF) with some polygonal (equiaxed) ferrite in a large columnar grains separated by grain boundary (allotriomorphic) ferrite (Fig. 9a) in the arc zone (approx. 10-15% penetration depth) in a wide range of heat inputs as presented in Fig. 7a, where experiments are sorted with declination

of AF amount and this also applicable Fig. 7b, c, d. In the middle of fusion zone (50% penetration depth, Fig. 7b) some bainite occurs with increase of fraction of Widmanstätten ferrite (WF) (Fig. 9b) possessing low resistance to fracture. At 75% penetration depth (see Fig. 7c) most of welds still possess fairly large amount of AF potentially providing acceptable toughness results despite of large amount of bainite was formed. At the root of weld (95% penetration depth, Fig. 7d) bainitic transformation with small fraction of martensite was commonly observed probably related to the difficulty of filler wire delivery from the arc and increased higher cooling cycles due to large heat sink of thick plates. The fraction of developed AF has very limited relation to any welding parameter except torch arrangement where more AF is formed in leading torch throughout a whole penetration depth probably related to more favorable melt flow at the range of selected welding parameters.

As an example, developed microstructures of weld No. 9 are presented in Fig. 8. At the root more complex microstructure can be developed, similarly to Fig. 8e, where AF or WF plate can be infused by bainitic or martensitic matrix as shown in Fig. 9c (Bhadesia and Honeycombe, 2006). In this case, the developed plate is idiomorphic, growth inside prior austenite grain during solidification. Similar complex microstructures were reported by Ghomashchi et al. (2015) in X70 high strength low alloy (HSLA) welded with shielded metal arc welding process. The presence of ferrite plate, indicated by measured hardness not exceeding 300 HV, compared to measurement on bainitic microstructure reaching 320-350 HV. A developed microstructure in the weld provided acceptable toughness of 138 J average at - 50 °C however with fairly significant scattering of data (individual results are: 139 J; 228 J; and 46 J) considering that testing weld metal in easier in term of accurate location of the notch which is schematically shown in Fig. 12a.

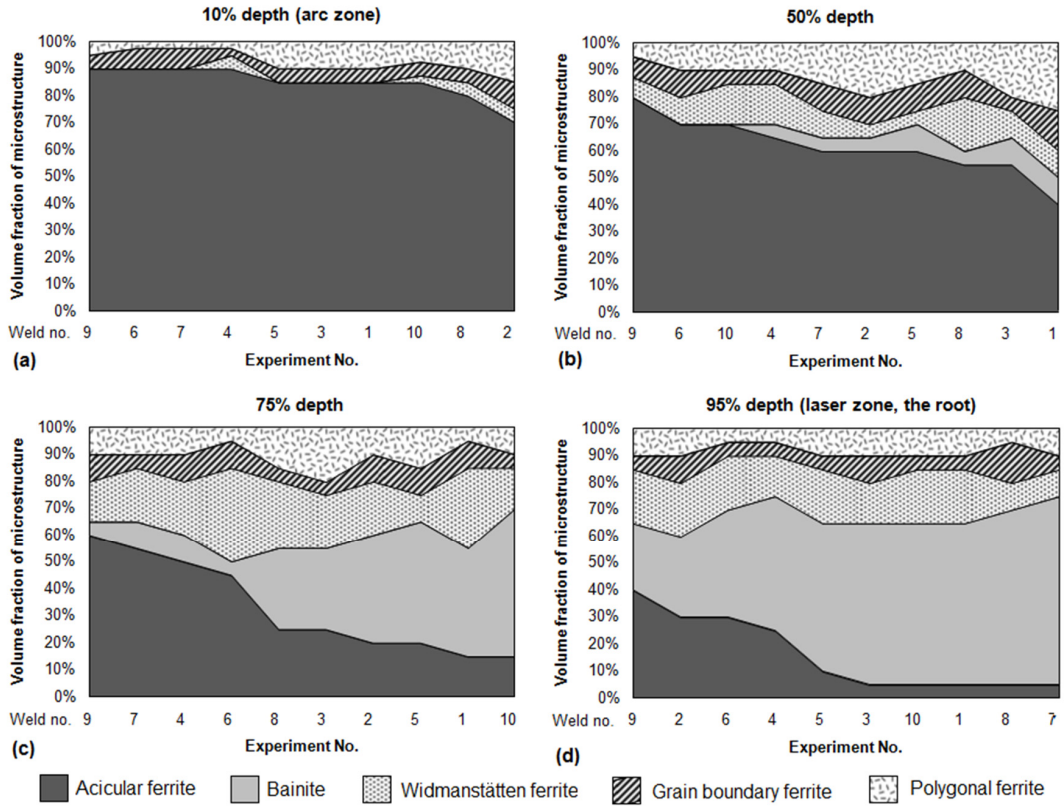

Fig. 7. Microstructural development in fusion zone (ordered in declination of AF fractions).

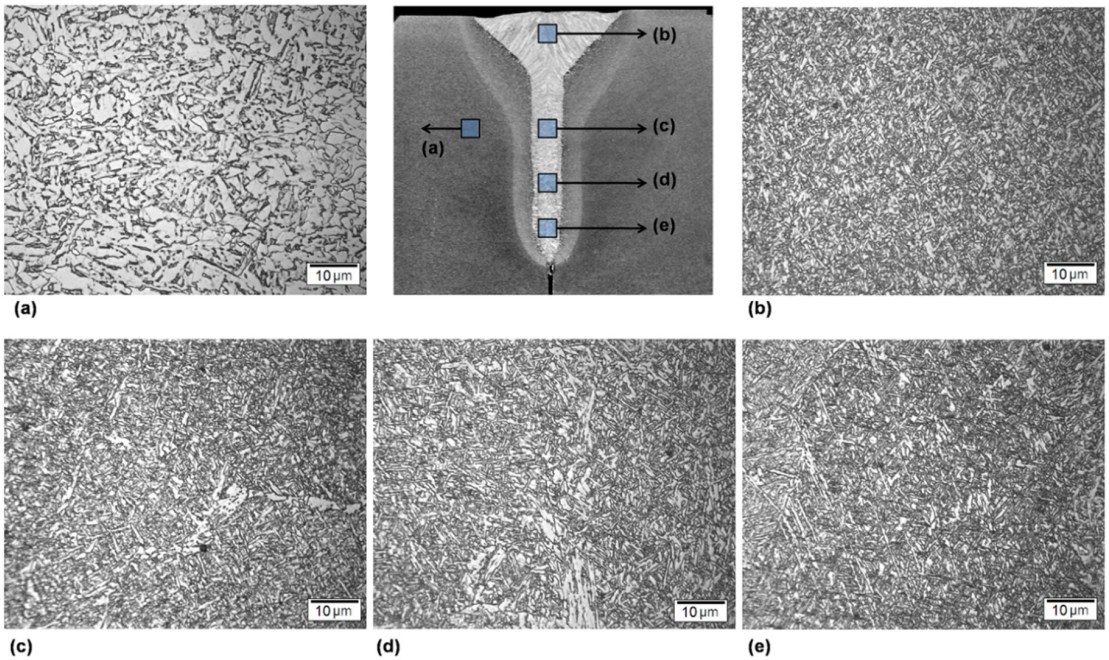

Fig. 8. Base material microstructure and microstructural development in fusion zone.

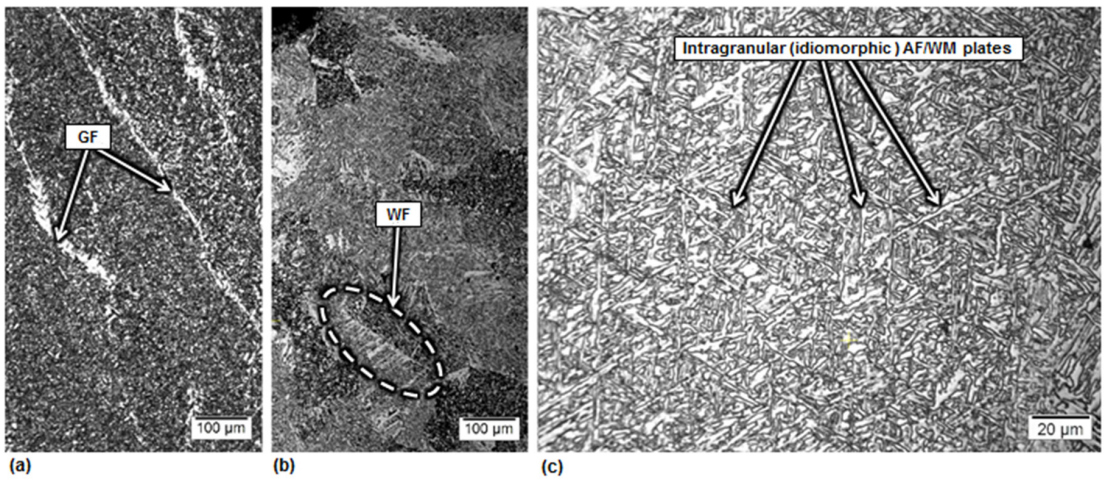

Fig. 9. (a) Grain boundary ferrite (GF) formation in the arc zone of weld metal which separates large columnar grains of welds and (b) WF formation in weld metal at 50% penetration depth and (c) example of complex microstructure at the root of weld (95% penetration depth).

In general, microstructural development results comply with hardness results presented in Fig. 11 as an indicator of particular microstructure. The upper part of weld (the arc zone) provides only slightly higher hardness (less than 20% increase) compared to base materials due to high fraction of AF possessing excellent mechanical properties and ductility. At the root, the hardness is significantly increased (by 50%) in weld metal and due to large fraction of bainite (upper) with possible some martensite overall with possible decreased toughness values. In the coarse-grained HAZ (CGHAZ) the hardness values are similar to the top part of the weld as shown in Fig. 11a, b possibly providing similar toughness.

CGHAZ development is very similar within same range of heat input regardless other welding parameters. Generally, the CGHAZ is fairly narrow at the top of weld (1.0-2.0 mm) and extremely narrow at the root (0.2-0.5

mm). Two specimens were selected for microstructural development of CGHAZ near fusion line, trailing CMT+P arc mode with 1.4 kJ/mm linear energy input (weld No. 7) and leading pulsed arc mode providing 1.7 kJ/mm (weld No. 8) with the same other welding parameters (0.4 mm air gap, 0.8 m/min travel speed, and 9 m/min *WFR*) and presented in Fig. 10. At low heat input (1.4 kJ/mm), CGHAZ possess less coarseness of grains than higher heat input weld (1.7 kJ mm) due to slightly shorter cooling cycles consisting of predominantly various ferritic phases (e.g. ferrite with aligned secondary phase (FS), WF, and low amount of AF including small fraction of upper bainite). As a result, hardness values are slightly higher (see Fig. 11). The same tendency complies in middle part of the welds. At the root, despite the same trend for hardness values, the grain size is nearly the same (Fig. 10c and Fig. 10f) and that implies the grain size is slightly affected by overall heat input.

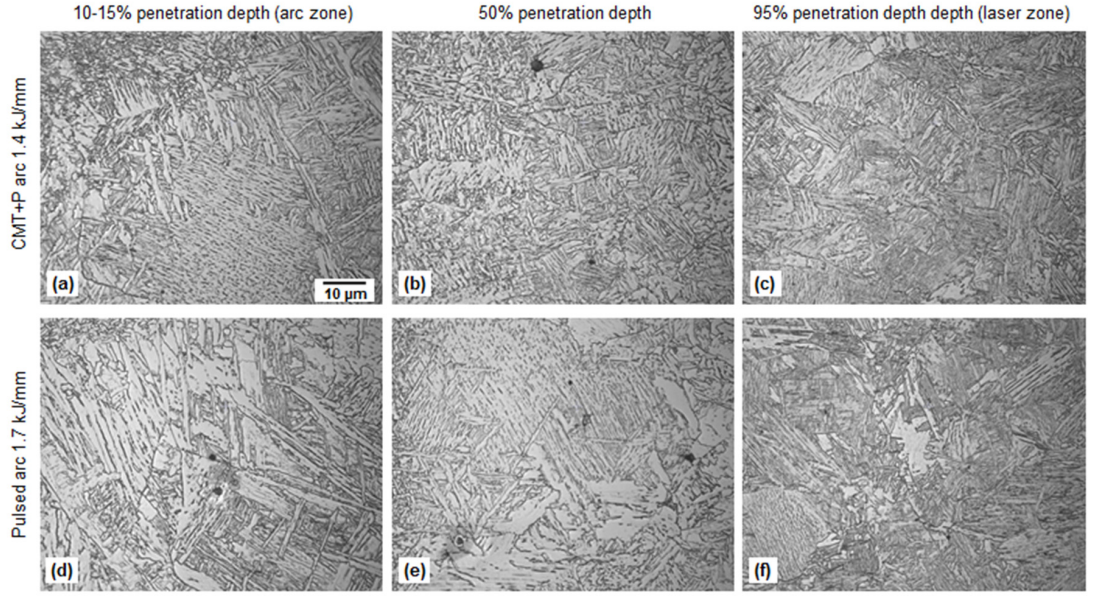

Fig. 10. Microstructural development in CGHAZ near fusion line of (a) low line energy output (CMT+P arc) and (d) high line energy output (Pulsed arc).

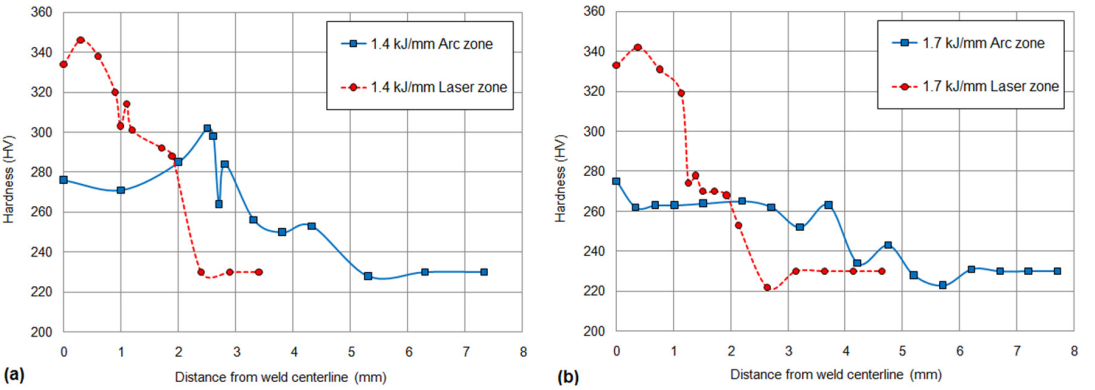

Fig. 11. Hardness measurements results: a) CMT+P arc (weld No. 7); b) Pulsed arc (weld No. 8).

Charpy V-notch test obtained values for fusion line are presented in Fig. 12. Notches were prepared at the fusion line (narrow area between CGHAZ) and weld metal as shown in Fig. 12a. According to the Charpy V-notch toughness results fairly good toughness can be achieved -50 °C temperature.

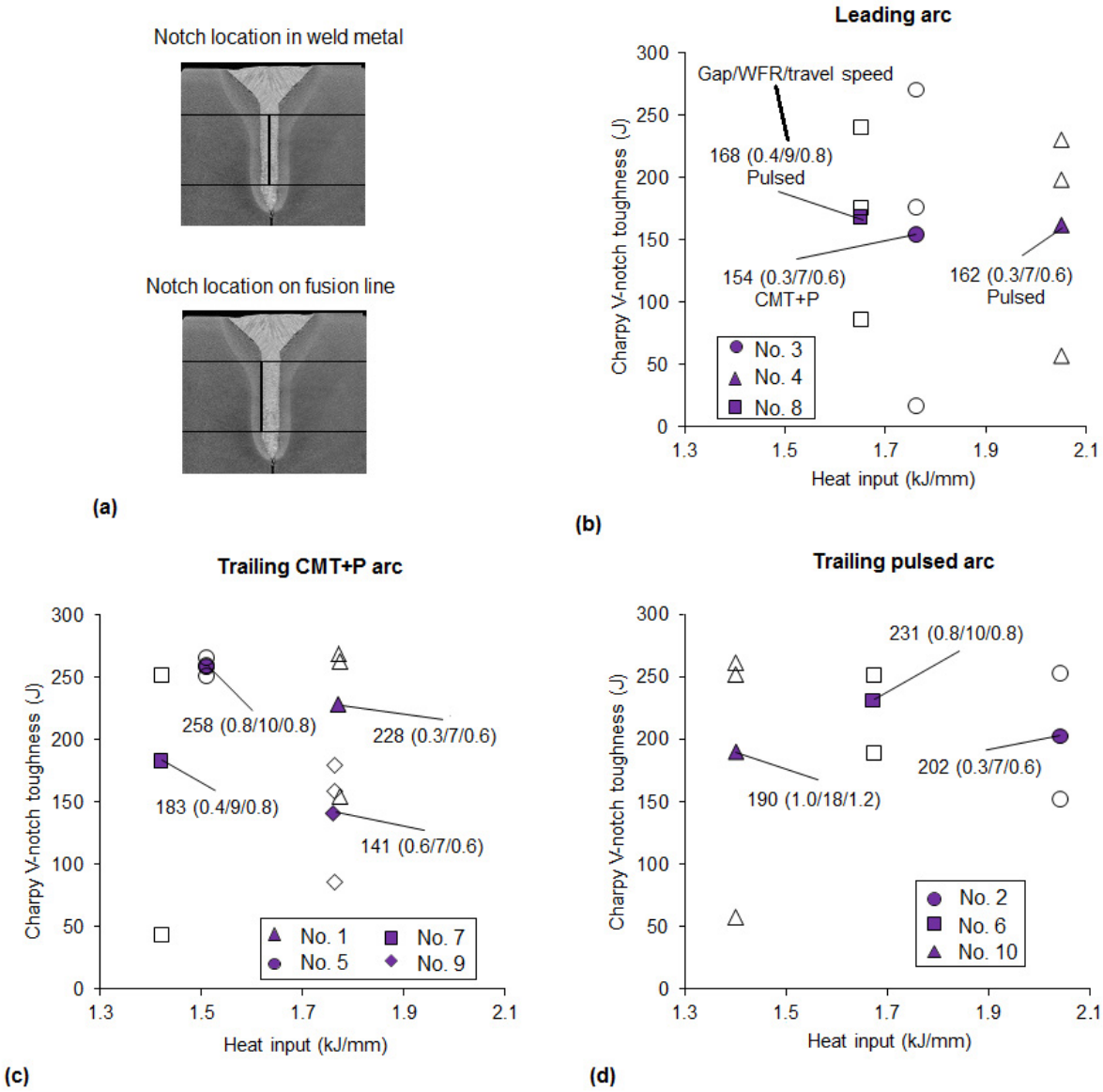

Fig. 12. Charpy V-notch toughness results of laser-GMA weld tested at -50°C where filled marks shows average values (of the 3 tested specimens) and no filled marks are individual values.

3.3. Concluding remarks

According to Fig. 12 heat input values has low relation to the obtained toughness values. CMT+P arc mode did not provide better toughness results with lower heat input potentially having lower distortions with reduced residual stresses. The developed microstructure near fusion line and other selected welding parameters involved has no direct link to the toughness results since the developed crack can be deflected from starting position (located at fusion line) to CGHAZ or weld metal and significant scattering of the toughness results. As a result, correlation between microstructural development, hardness and toughness was not possible to establish due to scattering. More in-depth testing, such as crack-tip opening displacement (CTOD), should be conducted on this matter in future research.

4. Conclusions

Thick high strength steel plates have been shown to be efficiently joined up to 40 mm thickness with appropriate toughness results at -50 °C with LAHW by applying double-sided welding technique and a few conclusions can be drawn:

- CMT+P arc mode is not recommended to be applied for travel speeds higher than 0.8 m/min due to specific metal-cored wire instabilities (wire chopping) caused by very short arc length which can result in poorer quality of welds such as spattering or macro-porosity.
- Torch arrangement has a significant influence on process stability. Leading torch setup has unfavourable droplet flight path trajectory since they can impinge the keyhole opening area and introduce porosity in welds.
- An increase of air gap, with correspondingly increased filler wire feed rate, can significantly increase process efficiency (penetration depth), which can be further increased by having a trailing torch arrangement when Pulsed arc mode is applied.
- Acicular ferrite can be formed throughout up to 75% depth of weld fusion zone in a fairly large amount (30-40%) with appropriate welding technique and optimized welding parameters by hybrid welding offering much higher productivity than arc welding processes.
- Toughness results are not significantly affected by heat input in the 1.4-2.1 kJ/mm range. Scattering in toughness can be related to difficulties in accurately locating notch for Charpy V-notch testing. This implies necessity to perform CTOD testing for more reliable correlation of the results.

Acknowledgements

The authors wish to thank the Research Council of Norway for funding through the Petromaks 2 Programme, Contract No.228513/E30. The financial support from ENI, Statoil, Lundin, Total, JFE Steel Corporation, Posco, Kobe Steel, SSAB, Bredero Shaw, Borealis, Trelleborg, Nexans, Aker Solutions, FMC Kongsberg Subsea, Marine Aluminium, Hydro and Sapa are also acknowledged.

References

Akselsen, O.M., Wiklund, G., Østby, E., Sørgjerd, A., Kaplan, A., 2013. A First Assessment of Laser Hybrid Welding of 420 MPa Steel For Offshore Structure Applications. In Proceedings of the 14th Nordic Laser Materials Processing Conference (NOLAMP), August 26-28th. Gothenburg, Sweden. Luleå University of Technology. p. 171-182.

Bhadesia, H. K. D.H., Honeycombe, 2006. Steels: Microstructure and Properties. 3rd ed. Butterworth-Heinemann, p. 155-164

Frostevarg, J., Kaplan, A.F., Lamas, J., 2014. Comparison of CMT with other arc modes for laser-arc hybrid welding of steel. Welding in the World 58 (5), p. 649-660

Ghomashchi, R., Costin, W., Kurji, R., 2015. Evolution of weld metal microstructure in shielded metal arc welding of X70 HSLA steel with cellulosic electrodes: A case study. Materials Characterization 107, p. 317-326

Gook, S., Gumenyuk, A., Rethmeier, M., 2014. Hybrid laser arc welding of X80 and X120 steel grade. Science and Technology of Welding and Joining 19(1), p. 15-24

Grünenwald, S., Seefeld, T., Vollertsen, F., Kocak, M., 2010. Solutions for joining pipe steels using laser-GMA-hybrid welding processes. Physics Procedia5 (Part B), p. 77-87.

Moore, P.L., Howse, D.S., Wallach, E.R., 2004. Microstructures and properties of laser/arc hybrid welds and autogenous laser welds in pipeline steels. Science and Technology of Welding and Joining 9(4), p. 314-322

Ono, M., Shinbo, Y., Yoshitake, A., Ohmura, M., 2002. Development of Laser-arc Hybrid Welding. NKK Technical Review No. 86, p. 8-12

Pan, Q., Mizutani, M., Kawahito, Y., Katayama, S., 2016. High power disk laser-metal active gas arc hybrid welding of thick high tensile strength steel plates. Journal of Laser Applications 28, 012004; doi: 10.2351/1.4934939

Pang, J., Hu, S., Shen, J., Wang, P., Liang, Y., 2016. Arc characteristics and metal transfer behavior of CMT+P welding process. Journal of Materials Processing Technology 238, p. 212-217

Sugino, T., Tsukamoto, S., Nakamura, T., Arakane, G., 2005. Fundamental Study on Welding Phenomena in Pulsed Laser-GMA Hybrid Welding. In Proc. of 24th International Congress on Applications of Lasers and Electro-Optics (ICALEO), 31th October to 3rd November. Miami, Florida, USA. Laser Institute of America, p. 108-116

Svensson, L-E., Gretoft, B., 1990. Microstructure and Impact Toughness of C-Mn Weld Metals. Welding Journal, 69(12), p. 454-461